

Gamma-Hadron Separation using Čerenkov Photon Density Fluctuations

V. R. Chitnis and P. N. Bhat*

*Tata Institute of Fundamental Research,
Homi Bhabha Road, Mumbai 400 005, India.*

Abstract. In the atmospheric Čerenkov technique γ - rays are detected against the abundant background produced by hadronic showers. In order to improve the signal to noise ratio of the experiment, it is necessary to reject a significant fraction of hadronic showers. Traditional background rejection methods based on image shape parameters have been extensively used for the data from imaging telescopes. However, non-imaging Čerenkov telescopes have to develop very different means of statistically identifying and removing cosmic ray events. Some of the parameters which could be potentially important for non-imaging arrays are the temporal and spectral differences, the lateral distributions and density fluctuations of Čerenkov photons generated by γ - ray and hadron primaries. Here we study the differences in fluctuations of Čerenkov photon density in the light pool at the observation level from showers initiated by photons and those initiated by protons or heavier nuclei. The database of simulated events for the PACT array has been used to evaluate the efficiency of the new technique. Various types of density fluctuations like the short range and medium range fluctuations as well as flatness parameter are studied. The estimated quality factors reflect the efficiencies with which the hadrons can be rejected from the data. Since some of these parameters are independent, the cuts may be applied in tandem and we demonstrate that the proton rejection efficiency of $\sim 90\%$ can be achieved. Use of density fluctuations is particularly suited for wavefront sampling observations and it seems to be a good technique to improve the signal to noise ratio.

Keywords: VHE γ - rays, Extensive Air Showers, Atmospheric Čerenkov Technique, Simulations, CORSIKA, Čerenkov photon density, density fluctuations, gamma-hadron separation.

1. Introduction

The atmospheric Čerenkov technique has become an increasingly mature experimental method of very high energy (VHE) γ -ray astronomy in the recent years (Weekes , 1988; Cronin, Gibbs, and Weekes , 1993; Cawley and Weekes , 1995; Aharonian and Akerlof , 1997; Ong , 1998; Catanese and Weekes , 1999). Major effort has gone into the optimization of γ -hadron separation(Fegan , 1997; Chitnis and Bhat , 2001), the energy calibration, energy resolution (Hofmann *et al.*, 2000)

* pnbhat@tifr.res.in



and the evaluation of spectra of γ -ray sources. Both imaging and non-imaging techniques play an increasingly important role in measuring the precise spectra of TeV γ -ray sources over a wide energy range (Aharonian *et al.*, 2001; Arqueros *et al.*, 2002; Oser *et al.*, 2001; De Naurois *et al.*, 2002). Among the non-imaging telescopes are the detector arrays based on solar concentrators like the CELESTE, GRAAL and STACEE have the potential to achieve unprecedented low energy thresholds for ground based γ -ray detectors (Dumora *et al.*, 1996; Arqueros *et al.*, 1997; Ong *et al.*, 1995). The imaging technique is also evolving with several large (10 m class) imaging telescopes forming a stereoscopic array to achieve unprecedented angular resolution *e.g.* HESS(Aharonian *et al.*, 1997), VERITAS(Weekes *et al.*, 1996b). These are currently under development. A single large imaging telescope (17 m diameter) is also under development which could achieve the lowest ever threshold of $\sim 10 GeV$ for primary γ -rays (Blanch *et al.*, 1998).

However, there has been a major difficulty in applying the atmospheric Čerenkov technique successfully for γ - ray astronomy. The abundant charged cosmic ray particles generate Čerenkov light akin to that produced by the γ - rays as a result of which the γ - ray signal is buried in a vast sea of cosmic ray background. Accurate location of the direction from which the primary particle is incident at the top of the atmosphere has been an important feature of successful observations since hadronic showers are isotropic. This has been the motivation to develop very good angular resolution capabilities (Majumdar *et al.*, 2002). But since γ -ray sources are weak one needs additional methods to reject the on-axis hadronic showers from the data. Such techniques have been developed for imaging telescopes (Fegan , 1997) while they are still being developed for non-imaging telescope arrays (Chitnis and Bhat , 2001).

The best distinction between γ -ray and proton showers should be based on an ideal parameter that does not show large deviations from its mean value *i.e.* it has a narrow distribution, and also whose fitted γ -ray curve should be well separated from the corresponding one for the hadronic showers. Often this is hardly achievable by using a single parameter and one often uses two or more parameters in tandem (Chitnis and Bhat , 2001) or simultaneously uses several parameters together with their correlations (Aharonian *et al.*, 1989) to achieve the same goal. Major difficulty is that these parameters often vary with primary energy and core distance, hence the separability too.

Methods for the efficient discrimination of photon and hadron initiated showers have been derived from the differences in the intrinsic properties of the Čerenkov radiation from pure electromagnetic and hadronic cascades. Differences manifest in the spatial as well as tempo-

ral distributions of the Čerenkov photons at the observation level. As a result, systematic studies of these photons as received at the observation level could lead to the development of techniques to distinguish between hadronic or photon primaries. There are several Atmospheric Čerenkov arrays designed precisely to apply these techniques to ground based VHE γ -ray astronomy (Dumora *et al.*, 1996; Arqueros *et al.*, 1997; Bhat, 1998; Ong, 1996; Ong and Covault, 1997; Tümer *et al.*, 1990).

The technique of separating proton or heavy nuclei initiated showers from γ -ray initiated showers was successfully developed first using atmospheric Čerenkov images (Fegan, 1997; Weekes, 1996a). A new method is based on the image surface brightness which seems to change with primary energy and species. This shows the importance of the photometric information of Čerenkov images in addition to the image shape parameters (Badran and Weekes, 1997) demonstrating that the photon densities too contain species dependent signature. More recently, a method based on the differences in the fluctuations of light intensity in the images of showers initiated by γ -rays and cosmic ray hadrons has been developed to offer additional background rejection capability (Bugayov *et al.*, 2002).

In the present work we similarly explore a new discrimination technique from a study of the spatial profile of Čerenkov light brightness from pure electromagnetic cascades as well as hadronic cascades generated by very high energy primaries. The technique is based on the differences in the intrinsic fluctuations in the Čerenkov photon densities at the observation level produced in the pure electromagnetic and hadronic cascades. The photon density fluctuations are classified in terms of their spatial extent, *i.e.* ‘short’, ‘medium’ and ‘long’ range and then parameterized. We then investigate the sensitivity of these three basic parameters to primary species. The relative merits of these parameters are compared in terms of the quality factors which are indicators of the efficiency with which showers of hadronic origin could be rejected in order to improve the signal to noise ratio of the data.

In §2 of this paper, details of simulations are given, followed by the definition of the figure of merit for discrimination between γ -rays and cosmic rays in §3. In §4, we define the three different parameters based on relative photon density fluctuations and study their core distance dependences. Then we present the quality factors derived for each of the parameters for various primary energies. The dependence of the quality factors on the telescope opening angle and incident angle of the primary at the top of the atmosphere are discussed in §5 & 6 respectively. The §7 contains results on the species dependence of the

quality factors. A brief discussion of the results is presented in §8 and conclusions are summarized in §9.

2. Simulations

CORSIKA (version 5.60), (Knapp and Heck , 1998; Heck *et al.*, 1998) has been used to simulate Čerenkov light emission in the earth's atmosphere by the secondaries of the extensive air showers generated by cosmic ray primaries or γ - rays. This program simulates interactions of nuclei, hadrons, muons, electrons and photons as well as decays of unstable secondaries in the atmosphere. It uses EGS4 code (Nelson , 1985) for the electromagnetic component of the air shower simulation and the dual parton model for the simulation of hadronic interactions at TeV energies. The Čerenkov radiation produced within the specified band width (300-650 nm) by the charged secondaries is propagated to the ground. The US standard atmosphere parameterized by Linsley (Linsley , 1962) has been used. The position, angle, time (with respect to the first interaction) and production height of each photon hitting the detector on the observation level are recorded.

In the present studies we have used Pachmarhi (longitude: $78^{\circ} 26'$ E, latitude: $22^{\circ} 28'N$ and altitude: $1075 m$) as the observation level where an array of Čerenkov detectors each of area¹ $4.35 m^2$ is deployed in the form of a rectangular array. We have assumed 17 detectors in the E-W direction with a separation of $25 m$ and 21 detectors in the N-S direction with a separation of $20 m$, making a total of 357 detectors deployed over an area of $400m \times 400m$. This configuration, similar to the Pachmarhi Array of Čerenkov Telescopes (PACT; figure 1)(Bhat , 1998) but much larger, is chosen so that one can study the core distance dependence of various observable parameters. Primaries consisting of γ - rays, protons, He and iron nuclei incident vertically on the top of the atmosphere are simulated in this study and have a fixed core position which is chosen to be the detector at the centre of the array. The resulting Čerenkov pool is sampled by all the 357 detectors which are used to study the core distance dependence of the parameters studied here. All the telescopes are assumed to have their optic axes aligned vertically. From practical considerations PACT has been divided into 4 sectors each of 6 telescopes. The physical size of a sector is approximately $20 m \times 50 m$ or $25 m \times 40 m$ depending on the orientation. In simulation however, there are 56 such sectors or 12 PACT like arrays (comprising 4 sectors) in the larger simulated

¹ This is the total reflective area of 7 parabolic mirrors of diameter $0.9 m$ deployed par-axially on a single equatorial mount.

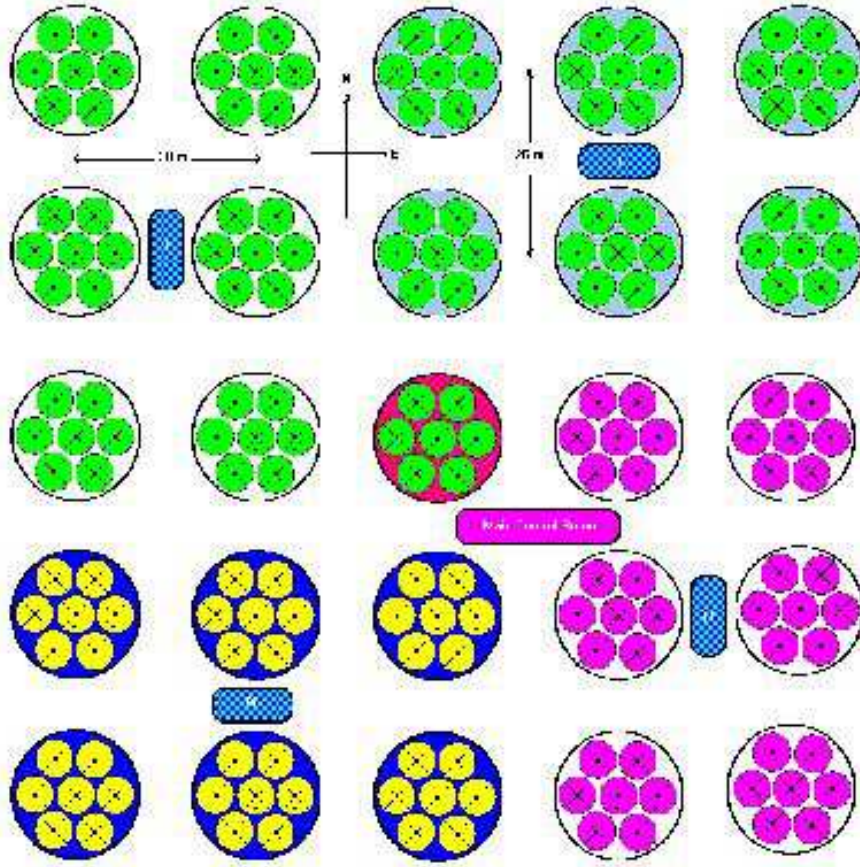


Figure 1. The PACT array showing the approximate positions of the 25 telescopes covering an area of about $80m \times 100m$.

array of 357 detectors. These are used for computing the density based parameters and study their core distance dependences.

An option of variable bunch size of the Čerenkov photons is available in the package which serves to reduce the requirement of hardware resources. This basically defines a maximal number of Čerenkov photons that are treated together as single entity. However since we are interested in the fluctuations of each of the estimated observables, we have tracked single photons for each primary at all energies. Multiple scattering length for electrons and positrons is decided by the parameter STEPC in the EGS code which has been set to 0.1 in the present studies (Ford and Nelson , 1978). The wavelength dependent absorption of Čerenkov photons in the atmosphere is not however taken into

account. The present conclusions are not expected to be dependent on photon wavelengths (Rahman *et al.*, 2001).

3. Figure of merit of a parameter

The figure of merit of a parameter that can distinguish between VHE γ -rays and cosmic ray hadrons depends primarily on two factors. Firstly, it should accept most of the γ -rays and secondly it should be able to reject most of the hadrons. We define such a figure of merit which is often called as *quality factor*, as (Chitnis and Bhat, 2001; Roberts *et al.*, 1998):

$$q = \frac{N_a^\gamma}{N_T^\gamma} \left(\frac{N_a^{cr}}{N_T^{cr}} \right)^{-\frac{1}{2}} \quad (1)$$

where N_a^γ is the number of γ rays accepted, N_T^γ is the total number of γ rays, N_a^{cr} is the number of background cosmic rays accepted and N_T^{cr} is the total number of background cosmic rays.

The quality factor thus defined is independent of the actual number of γ -rays and protons recorded. This is slightly different from the Q-factor generally used to measure improvement in the signal to noise ratio after applying cuts based on Čerenkov image shapes and orientation (Badran and Weekes, 1997).

4. Types of fluctuations

4.1. LOCAL DENSITY FLUCTUATIONS

Local density fluctuations (LDF) are defined as the ratio of the RMS variations to the mean number of photons in the 7 mirrors of a telescope. In the particular configuration chosen in the present study, the 7 mirrors form a compact pattern. Hence LDF, in this context, represents the short range (~ 1 m) photon jitter. Here we try to compare LDF's for γ -ray primaries *vis-a-vis* hadronic primaries and see if there is any tangible difference which could in-turn be used to discriminate the hadronic background.

4.1.1. Lateral Distribution of LDF

We have computed the LDF for each of 357 detectors for γ -ray and proton primaries whose energies at the top of the atmosphere are chosen such that they have comparable Čerenkov yield on the ground. Figure

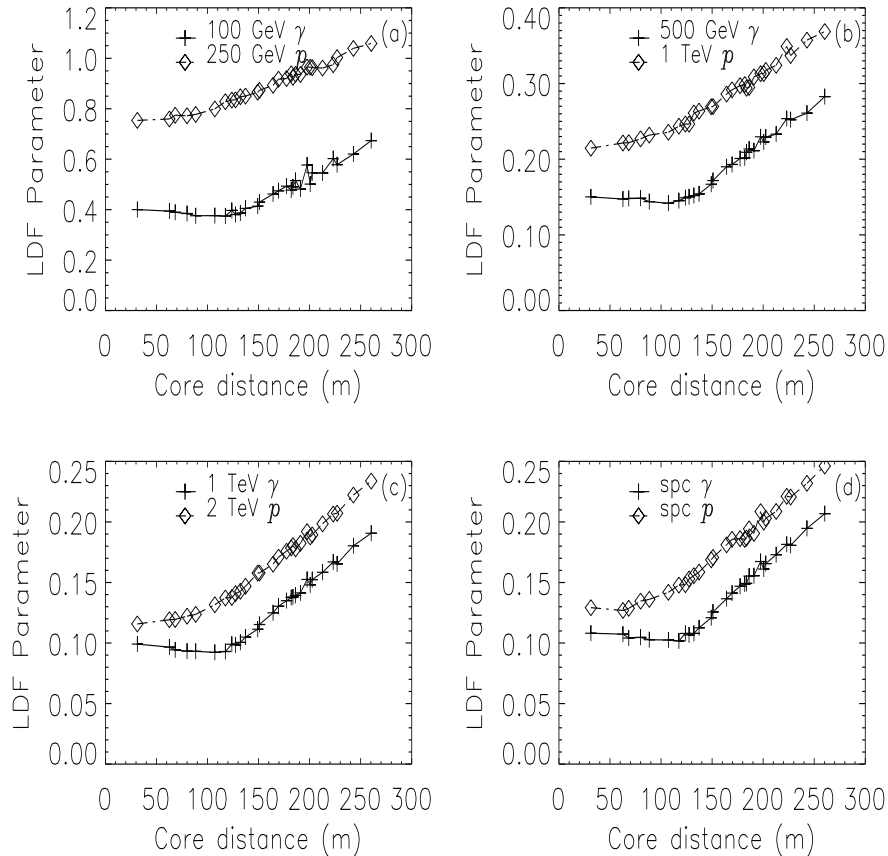


Figure 2. Radial variations of LDF averaged over 100 showers each for γ -ray (plus) and proton (diamonds) primaries of energies (a) 100 GeV & 250 GeV (averaged over 300 showers each) (b) 500 GeV & 1 TeV and (c) 1 TeV & 2 TeV respectively. Each set of energies for γ -ray and proton energies are chosen such that they have comparable Čerenkov yield. Panel (d) shows similar distributions for γ -rays & protons of primary energies randomly chosen from a power law spectrum of slope -2.65 (see text for details).

2 shows the radial variations of mean LDF both for γ -rays and protons for three pairs of primary energies as shown. The panels *a*, *b* and *c* show the radial variation of LDF for mono-energetic primaries while panel *d* shows the same when the energies of the primary are picked randomly from a differential power law spectrum (within the energy band of 0.5 - 10 TeV for γ -rays and 1 - 20 TeV for protons) of slope -2.65. One can readily see that LDF increases smoothly with increasing core distance for both γ -ray and proton primaries beyond the hump distance of about 130 m at this observation level (Chitnis and Bhat ,

1998). LDF for proton primaries is distinctly higher than that for γ -rays at all primary energies considered here while their absolute values as well as their separations decrease with increasing primary energy as expected (Chitnis and Bhat , 1999).

4.1.2. Quality Factors using LDF

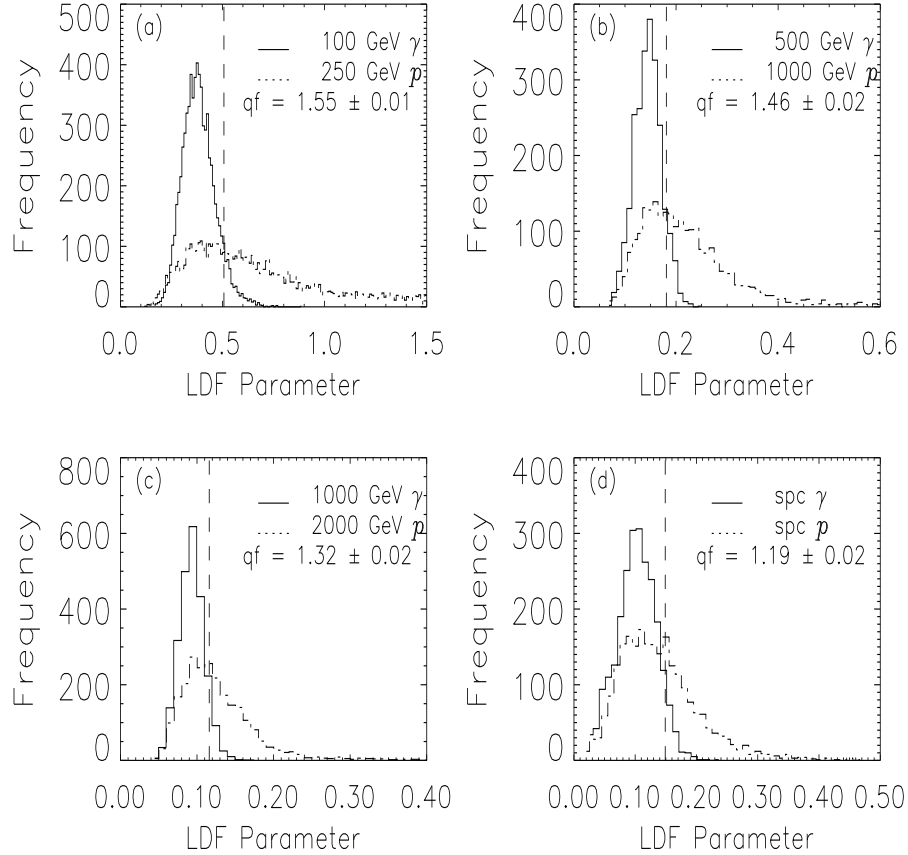


Figure 3. Distributions of LDF for γ -ray and proton (dotted line) primaries of three sets of energies as in figure 2. The dashed vertical lines show the threshold values chosen to yield maximum quality factors in each case. The number of showers used are same as those mentioned in figure 2.

Figure 3 shows the distributions of LDF's for γ -ray and proton primaries of various energies incident vertically at the top of the atmosphere. The distributions for proton primaries are more skewed compared to those of γ -rays and hence result in good quality factors. The widths of the distributions for both types of primaries decrease with

Table I. Quality factors derived using local density fluctuations for primaries of various energies incident vertically at the top of the atmosphere.

Primary Energy	Threshold LDF	Quality Factor	Fraction Accepted
100 GeV γ -rays and 250 GeV protons	0.51	1.55 ± 0.01	0.922 0.355
500 GeV γ -rays and 1 TeV protons	0.18	1.46 ± 0.02	0.880 0.364
1 TeV γ -rays and 2 TeV protons	0.12	1.32 ± 0.02	0.872 0.435
Spectrum of γ -rays and protons	0.15	1.19 ± 0.02	0.91 0.59

increasing energy and their relative separations too decrease. The vertical dashed lines show the threshold values chosen to yield maximum quality factors and retain atleast 30% γ -ray signal. Only detectors within a core distance of 150 m are used in these distributions.

Table I shows the quality factors estimated using LDF as a parameter for the same primary energies of γ -rays and protons shown in figure 2. The second column shows the threshold LDF values such that the showers whose LDF values are above this are discarded yielding a quality factor shown in column 3. The column 4 lists the fraction of the γ -ray and proton events retained in the process. The quality factors decrease steadily with increasing primary energies probably because the intrinsic fluctuations are smoothed out at higher primary energies. This is consistent with the radial variations shown in figure 2. In addition, the threshold LDF values decrease with increasing primary energies since the value of LDF's also decrease with energy.

The lateral distributions of γ -rays and hadrons are distinctly different within the hump distance of about 130 m (Chitnis and Bhat , 1998). The γ -ray lateral distribution is relatively flat until the hump distance and then falls while that for proton primaries it falls monotonically right from the core. This difference in the lateral profile could very well give rise to differences in the LDF values for the two primaries as shown in figure 3. Hence LDF could arise purely out of the Poisson

fluctuations of the number of Čerenkov photons incident on each of the 7 mirrors. When the quantity $\frac{1}{\sqrt{n(r)}}$ is plotted as a function of core distance, (where $n(r)$ is the number of Čerenkov photons incident on a mirror at a core distance r) it coincided with that shown in figure 2 demonstrating that LDF does not contain any non-Poissonian fluctuations. Hence the modest quality factors arise due to the differences in the lateral distributions. This shows that the kinematical differences in the cascade development by primary γ -rays and protons give rise to only long range fluctuations.

4.2. MEDIUM RANGE DENSITY FLUCTUATIONS

Medium range density fluctuation (MDF) is defined as the ratio of the RMS variations of the total number of photons detected in each of the 6 telescopes² in a sector to the average number of photons incident on a telescope. In other words, MDF is a measure of the variation of Čerenkov photons over a medium range of $\sim 50 m$. As mentioned before, we have 56 independent sectors in the large array chosen in our simulation, situated at various core distances.

4.2.1. Lateral Distribution of MDF

Figure 4 shows the radial variation of MDF for the same four pairs of energies for γ -rays and protons as in the case of LDF. It can be seen that the MDF values of γ -rays and protons are separated at lower primary energies showing that it can well be used as a parameter to distinguish between them. The MDF values for proton primaries are less sensitive to the core distance as compared to LDF values at almost all primary energies. However the γ -ray primaries exhibit a prominent peak around the hump region especially at higher energies. The maximum MDF could exceed that for protons at energies $\geq 2 TeV$. The absolute values of MDF decrease with increasing primary energies as in the case of LDF.

4.2.2. Quality Factors using MDF

Figure 5 shows the distributions of MDF for both γ -ray and proton primaries of various energies as indicated. The quality factors are listed in table II, the format of which is same as that of table I. It can be seen from table II that the quality factors based on MDF as a parameter fall with increasing energy. The threshold values too decrease with increasing primary energy as in the case of LDF. The fraction of accepted

² which is the sum of the photons incident on all the 7 mirrors constituting the telescope.

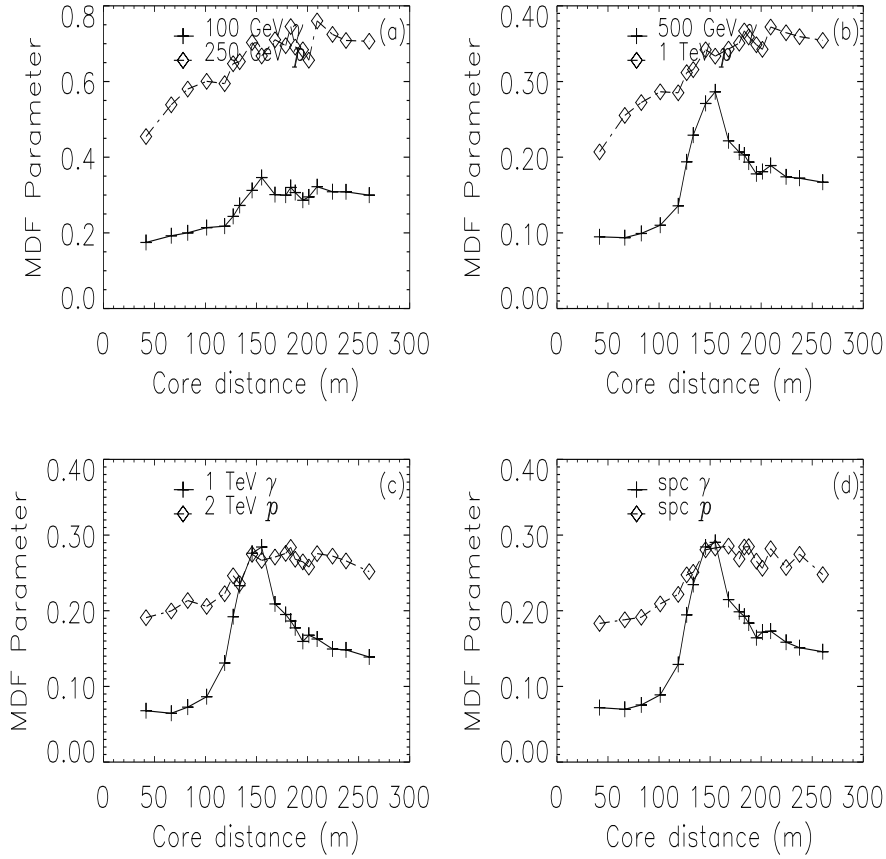


Figure 4. Radial variations of MDF for γ -ray (plus) and proton (diamonds) primaries. The rest of the details are same as in figure 2. The number of showers used are 300 each in panel a and b while it is 100 each for γ -rays and protons for the rest.

γ -rays falls more steeply while the fraction of protons rejected increases with increasing primary energy unlike LDF. The former is due to the progressive increase in MDF for γ -ray primaries around the hump region with increasing energy. We have included only those showers with core distances less than 150 m while estimating these quality factors. In a wavefront sampling experiment like PACT₂, it is possible to estimate the core position from a spherical fit to the Čerenkov light front (Chitnis and Bhat, 2002).

It has been seen that the differences in the MDF values of γ -ray and proton primaries is indeed due to intrinsic differences in the interaction characteristics of the primary species in the atmosphere unlike

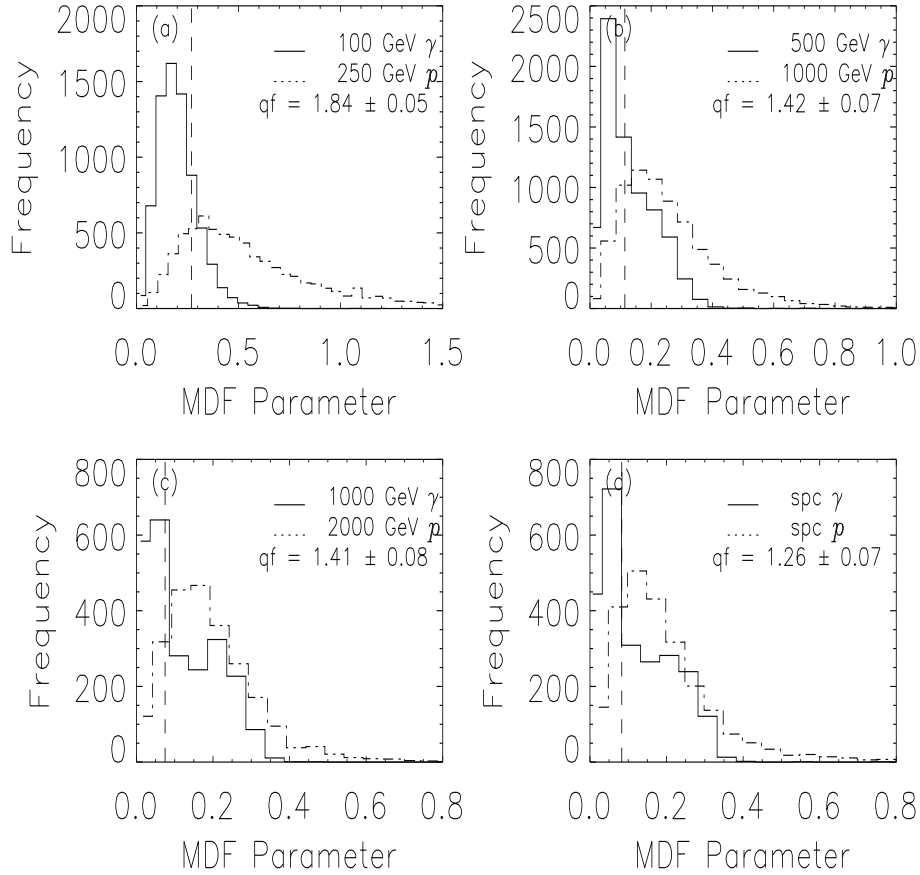


Figure 5. Distributions of MDF for γ -ray and proton (dotted line) primaries of three sets of energies as in figure 2. The dashed vertical lines show the threshold values chosen to yield maximum quality factors in each case. The number of showers simulated in each case are same that mentioned in the caption of figure 4.

LDF. This conclusion has been arrived at by computing the quality factors after removing the contribution to MDF from pure statistical (Poissonian) fluctuations.

4.3. FLATNESS PARAMETER

Flatness parameter is a quantity α defined below, which is proportional to the average variance of the total number of Čerenkov photons incident on each of the 24 telescopes over the 4 sectors. It is a long range parameter which represents a measure of smoothness of the lateral distribution of Čerenkov photons generated by γ -rays and protons. It is defined as (Vishwanath , 1993):

Table II. Quality factors from medium range density fluctuations for primaries of various energies incident vertically at the top of the atmosphere.

Primary energy	Threshold MDF	Quality Factor	Accepted Fraction
100 GeV γ -rays and 250 GeV protons	0.27	1.84 ± 0.05	0.721 0.153
500 GeV γ -rays and 1 TeV protons	0.12	1.42 ± 0.07	0.478 0.109
1 TeV γ -rays and 2 TeV protons	0.08	1.41 ± 0.08	0.353 0.0625
Spectrum of γ -rays and protons	0.083	1.26 ± 0.07	0.37 0.086

$$\alpha = \frac{1}{N} \sum_{i=1}^N \frac{(\rho_i - \bar{\rho})^2}{\bar{\rho}} \quad (2)$$

where ρ_i is the total number of Čerenkov photons in the i^{th} telescope, while $\bar{\rho}$ is the mean ρ averaged over N telescopes in all the 4 sectors, ($N = 24$ in the present case).

4.3.1. Lateral Distribution of the flatness parameter

Figure 6 shows the variation of mean α as a function of core distance. It can be seen from the figure that α is a core distance dependent parameter showing a better separation for γ -ray and proton primaries at lower primary energies. In addition, at large core distances and at higher primary energies its value becomes almost independent of the primary species. As a result, the sensitivity of α to primary species reduces at large core distances. This is primarily due to the similarity of the Čerenkov photon lateral distributions from the electromagnetic and hadronic cascades beyond the hump region. In addition, the number of photons reduces at large core distances and hence the species independent Poissonian fluctuations dominate.

4.3.2. Quality Factors using flatness parameter

Figure 7 shows the distributions of α for γ -ray and proton primaries of various energies. The distributions for proton primaries are often more

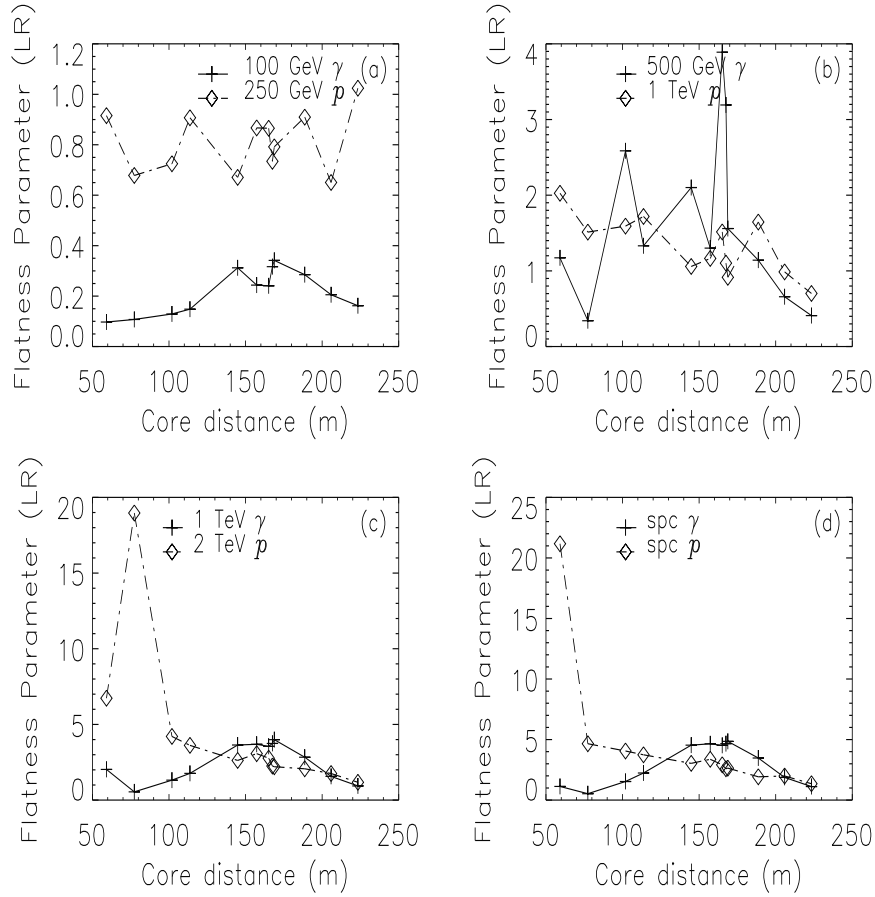


Figure 6. Radial variations of the mean flatness parameter (α) for γ -ray (plus) and proton (diamonds) primaries. α is averaged over 300 events each in panels (a) and (b) while it is averaged over 100 events each in panels (c) & (d). The rest of the details are same as in figure 2. The large fluctuations seen here are statistical.

skewed relative to that of γ -ray primaries. As a result, this parameter can be used to distinguish between the two types of primaries. The values of the quality factors estimated from these distributions for primaries of various energies are listed in table III. Also listed are the fraction of γ -rays and protons retained after rejecting showers with α values larger than the threshold values for each set of primary energies. The fraction of protons that are rejected by using α as a parameter increases rapidly with increasing energy reaching nearly 90% at higher energies. At the same time the fraction of γ -rays retained after rejection also decreases to $\sim 40\%$ at higher energies. The combined effect of the two energy dependent trends is that the quality factors decrease

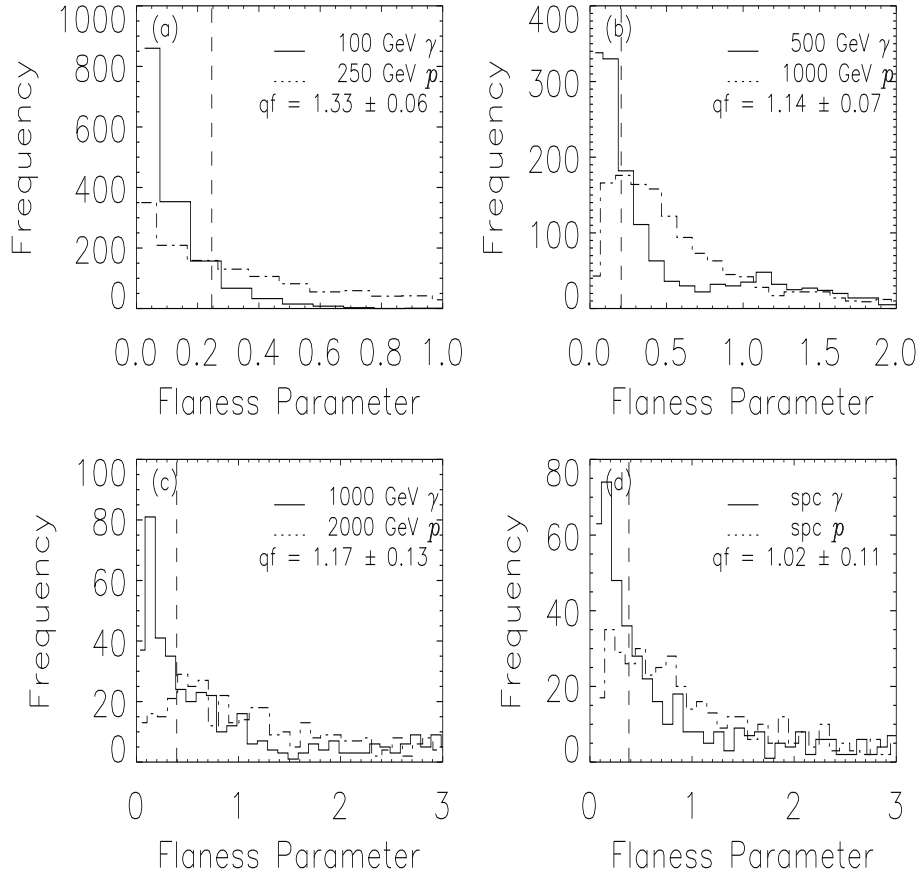


Figure 7. Distributions of the flatness parameter (α) for γ -ray (plus) and proton (diamonds) primaries of energies (a) 100 GeV & 250 GeV (b) 500 GeV & 1 TeV and (c) 1 TeV & 2 TeV respectively. Panel (d) shows similar distributions for γ -rays & protons of primary energies randomly chosen from a power law spectrum of slope -2.65 (see text for details). The dashed vertical lines show the threshold values chosen to yield maximum quality factors in each case. The number of showers simulated is same that in figure 6.

with increasing primary energy. A core distance cut of 150 m is used while estimating the quality factors.

α can be estimated for a single sector too (α_s). It has been found that this short range flatness parameter too behaves the same way as the 4-sector or long range flatness parameter except that the quality factors estimated using α_s are less by about 10%.

As mentioned before, α is a parameter proportional to the statistical variance of the total number of Čerenkov photons incident on each telescope of the array. Higher statistical moments like the skewness and

Table III. Quality Factors from the flatness parameter (α) for primaries vertically incident at the top of the atmosphere.

Primary Energy	Threshold α	Quality Factor	Accepted Fraction
100 <i>GeV</i> γ -rays and 250 <i>GeV</i> protons	0.25	1.33 ± 0.06	0.836 0.395
500 <i>GeV</i> γ -rays and 1 <i>TeV</i> protons	0.20	1.14 ± 0.07	0.397 0.121
1 <i>TeV</i> γ -rays and 2 <i>TeV</i> protons	0.4	1.17 ± 0.13	0.370 0.100
Spectrum γ -rays	0.38	1.02 ± 0.11	0.398 0.152

kurtosis too have been tested for their sensitivity to primary species. It was found that α is the most sensitive among them.

5. Effect of the telescope field of view on quality factors

The opening angle of a non-imaging Čerenkov telescope is generally limited by placing a circular mask at the focal point in front of the photo-cathode. This limits the arrival angle of the photons reaching the photo-cathode. In the absence of a mask the opening angle is limited by the photo-cathode diameter. In other words, the limiting mask is expected to prevent the arrival of photons at large angles. This effectively results in a reduction in the mean arrival time as well as an increase in the average production height of Čerenkov photons (Chitnis and Bhat, 2001). Table IV lists the quality factors (column 4) for each type of parameter (column 2) and the corresponding fractions of γ -rays (column 5) and protons (column 6) retained after applying the cuts as per the threshold values listed in column 2. The quality factors have been estimated for 4 different focal point mask diameters (column 1). The results are based on 100 showers each simulated for γ -rays and protons of primary energies 500 *GeV* and 1 *TeV* respectively. It may be noted from the table that the quality factors for all the three types of parameters improve with decreasing mask diameter without losing

γ -ray signal.³ This demonstrates that the primary species dependent differences in the three parameters arise mainly due to the intrinsic differences in the cascade development by the pure electromagnetic and proton primaries rather than the different angular distributions of Čerenkov photons at the observation altitude.

Table IV. Quality factors from density fluctuations for showers initiated by 500 GeV γ -rays and 1 TeV protons incident vertically at the top of the atmosphere when focal point masks of various sizes are used.

Mask diameter (FWHM)	Parameter	Threshold value	Quality factors	Accepted Fraction	
				γ -rays	Protons
5°	LDF	0.18	1.53 ± 0.02	0.838	0.302
	MDF	0.12	1.47 ± 0.07	0.471	0.103
	α	0.17	1.23 ± 0.09	0.334	0.074
4°	LDF	0.18	1.58 ± 0.02	0.843	0.285
	MDF	0.09	1.50 ± 0.09	0.347	0.053
	α	0.19	1.25 ± 0.15	0.350	0.078
3°	LDF	0.19	1.66 ± 0.03	0.885	0.285
	MDF	0.11	1.60 ± 0.09	0.437	0.075
	α	0.21	1.37 ± 0.16	0.382	0.078
2°	LDF	0.20	1.77 ± 0.03	0.709	0.160
	MDF	0.10	2.11 ± 0.17	0.308	0.021
	α	0.18	1.38 ± 0.19	0.302	0.048

In order to understand the effect of the focal point mask on the density parameters we will examine the radial variation of the components of one of the parameters (MDF) without and with a focal point mask in place, as shown in figures 8 and 9 respectively. From a comparison of the two figures, it can be easily seen that the mean photon densities fall more steeply when focal point mask is used while the standard deviation changes to a lesser extent. This effect is more pronounced for proton primaries than for γ -ray primaries. As a result, the MDF values increase relatively for proton primaries thus increasing the separation

³ This apparent improvement in quality factor is not due to fixed energies of protons and γ -rays. A similar improvement in quality factors was seen when the primary energies of protons and γ -rays were chosen randomly from a powerlaw spectrum of slope -2.65.

between the two species which in turn improve the quality factors when focal point masks are used, as observed above. Even though we take MDF as a typical example to illustrate the effect of focal point mask, the other parameters too are similarly affected qualitatively.

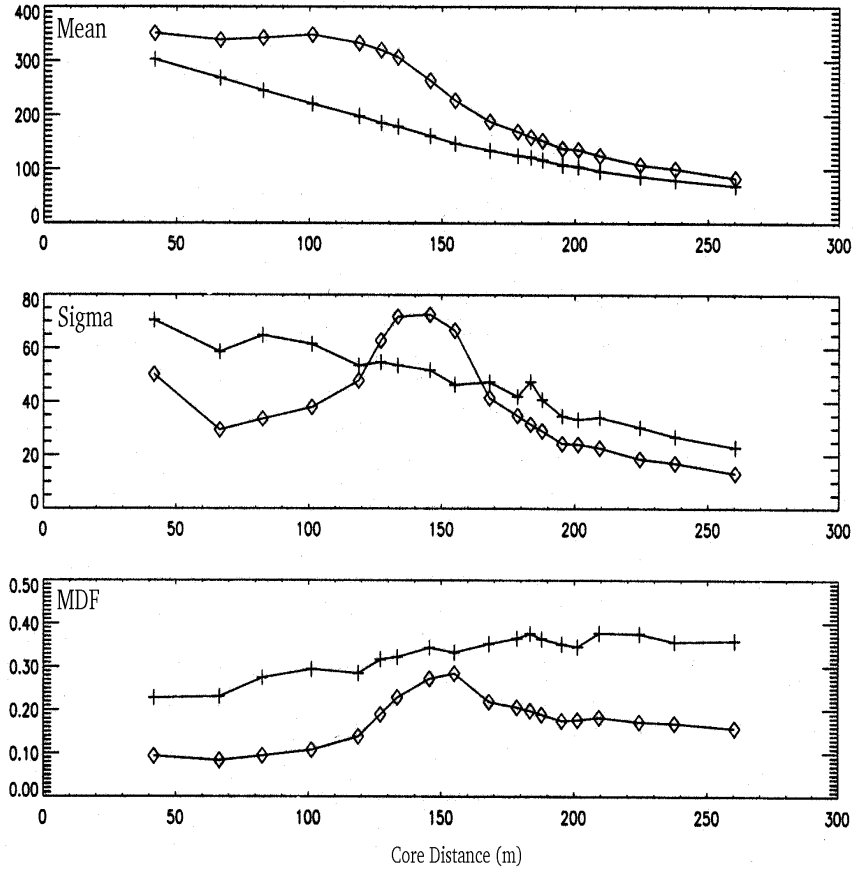


Figure 8. A plot of the radial variations of the mean photon density (top panel), standard deviation (middle panel) and MDF (bottom panel) when no focal point mask is used. The two curves in each panel correspond to γ -rays (diamond) of 500 GeV and protons (plus) of energy 1 TeV incident vertically at the top of the atmosphere.

6. Quality Factors for inclined showers

At larger zenith angles enhanced attenuation of Čerenkov light and increased distance from the shower maximum raise the energy thresholds of the primary that are detected by an atmospheric Čerenkov telescope.

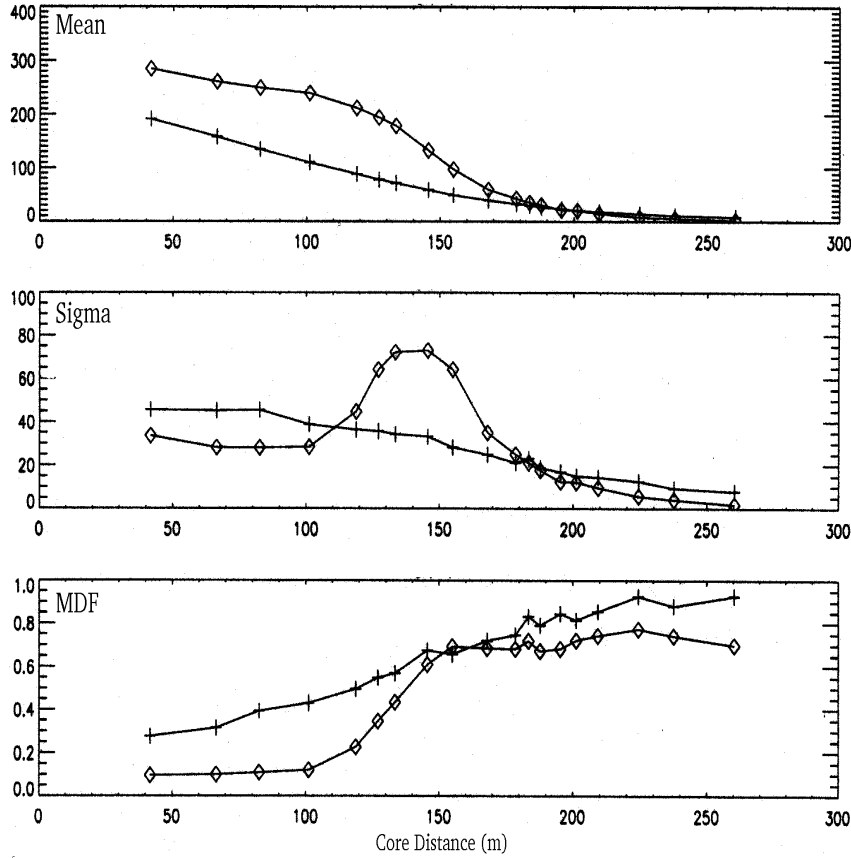


Figure 9. A plot of the radial variation of the mean value, standard deviation and MDF when a focal point mask of 4° (FWHM) is in place. The rest of the details are same as in figure 8.

After the shower maximum γ -ray induced showers attenuate progressively faster with atmospheric depth than do the hadronic showers. As a result one would expect a zenith angle dependence on the sensitivity of the parameters studied here. Qualitatively speaking inclined showers at a given altitude behave similar to vertical showers of same primary energy at a lower altitude. Consequently one would expect the quality factor to improve with zenith angle. Quality factors based on some of the timing parameters show an improvement at inclined direction (Chitnis and Bhat , 2001). The species sensitive imaging parameters like the azimuth on the other hand, have been shown to be much less sensitive for primaries incident at angles $\geq 30^\circ$ (Weekes *et al.*, 1989).

Table V summarizes the quality factors estimated for γ -ray and proton primaries of energy 500 GeV and 1 TeV respectively, incident at 30° to the vertical at the top of the atmosphere. These are based on 100 showers simulated for each type of primary. These quality factors when compared with those for vertical showers as listed in tables I, II and III show a marked improvement for α and MDF as parameters while it doesn't change significantly for LDF as a parameter.

Table V. Quality Factors estimated for 500 GeV γ -rays and 1 TeV protons incident at 30° to the vertical at the top of the atmosphere. The quality factors for three different parameters estimated with no focal point mask are shown.

Type of parameter	Threshold	Quality Factor	Accepted Fraction	
			γ -rays	Protons
α	0.35	3.28 ± 0.79	0.328	0.010
MDF	0.12	1.83 ± 0.08	0.617	0.113
LDF	0.22	1.39 ± 0.02	0.850	0.377

7. Quality Factors for heavy primaries

Each of the three species sensitive parameters under study here are applied to He and Fe primaries as well. Tables VI and VII summarize the results for 100 simulated showers each of 1 TeV γ -rays 2.5 TeV He and 10 TeV Fe nuclei incident vertically at the top of the atmosphere. The quality factors may be compared with those for protons as listed in tables I, II and III which show that both He and Fe nuclei may be more easily discriminated against γ -rays despite losing a higher fraction of γ -rays in the process. The fraction of cosmic rays retained after applying the cut is smaller in the case of heavier primaries for all the three density based parameters studied here.

8. Discussions

The subject of intrinsic inter-shower fluctuations has been dealt at length by Chitnis and Bhat (Chitnis and Bhat , 1998). Here what we are addressing is the techniques of exploiting intra-shower fluctuations in

Table VI. Quality Factors estimated for 1 TeV γ -rays and 2.5 TeV He nuclei incident vertically at the top of the atmosphere. The quality factors for three different parameters estimated with no focal point mask are shown.

Type of parameter	Threshold	Quality Factor	Accepted Fraction	
			γ -rays	He nuclei
α	0.57	1.11 ± 0.06	0.303	0.074
MDF	0.07	1.68 ± 0.12	0.312	0.035
LDF	0.11	1.46 ± 0.02	0.738	0.256

Table VII. Quality Factors estimated for 1 TeV γ -rays and 10 TeV Fe nuclei incident vertically at the top of the atmosphere. The quality factors for three different parameters estimated with no focal point mask are shown.

Type of parameter	Threshold	Quality Factor	Accepted Fraction	
			γ -rays	Fe nuclei
α	0.57	1.89 ± 0.15	0.301	0.025
MDF	0.07	2.23 ± 0.18	0.331	0.022
LDF	0.10	1.34 ± 0.02	0.659	0.243

Čerenkov photon density at the observation level. It is well known that in the case of hadronic primaries large fluctuations in the number of secondary particles created during the hadron multi-particle production is the main reason for larger fluctuations relative to that in photon primaries.

As can be seen from the tables I,II and III that the quality factors fall with increasing primary energy. This is consistent with our previous study (Chitnis and Bhat , 1998) where it was observed that the intra-shower density fluctuations decrease monotonically with increasing primary energy, thus reducing the distinguishability of γ -rays from protons. It may be interesting to note here that the fraction of protons rejected using these parameters increase with increasing primary energy at the cost of losing more γ -ray signal.

It has been seen in figures 2,4 and 6 that the Čerenkov photon density fluctuations are strong functions of the core distance as the photons received at various core distances are produced at different altitudes, *i.e.* at different stages in the cascade development (Hillas , 1996; Chitnis and Bhat , 1998). As a result, we see a dependence of the quality factors on the core distance. We have used a uniform cut of 150 m on the core distance in all the present studies (except for inclined showers since the Čerenkov light pool generated by them is azimuthally asymmetric) since no showers of primary energy $\leq 2 TeV$ with impact parameter above 150 m will generate a PACT trigger. However it is important to know the effect of this cut on the quality factors studied here. Figure 10 shows the variation of quality factors based on (a) α , (b) MDF and (c) LDF as a function of core distance cuts (increasing in units of 50 m , 0-50 m , 0-100 m *etc.*, shown as points) used for primary energies of 500 GeV and 1 TeV for γ -rays and protons respectively. The quality factors from α and MDF fall continuously when longer core distance events are included while that from LDF shows a maximum when the core distance cut is 150 m .

Also shown in the figure are the quality factors when only showers with differential impact parameter ranges 0-50 m , 50-100 m *etc.*, are included (histogram). The quality factors from MDF and α show a minimum for showers with impact parameters around the hump region (100-150 m for Pachmarhi altitude). This is primarily due to the fact that the absolute values of MDF and α exhibit minimum separation around the hump region as seen in figures 4 and 6 respectively. The quality factors based on LDF show a maximum in the same core distance range. This is a direct consequence of the hump in the case of γ -ray primaries.

In practice one can estimate the primary energy from which we can estimate the maximum possible core distance. This would enable us to make an optimum estimate of the nature of the primary. Alternately one can estimate the core position of each shower by using the curvature of the shower front (Chitnis and Bhat , 2002), as mentined before, which would help in deciding the optimum cut on the core distance for the data set.

If the three types of photon density based parameters investigated in the present study are independent,⁴ then one can use them in tandem to improve the hadron rejection efficiency even further, a procedure similar to the multi-dimensional shower image analysis (Aharonian *et*

⁴ LDF and MDF are expected to be independent since they use exclusive information content while α and MDF could be related. It has been found that the improvement resulting from the tandem application of α over and above LDF & MDF is marginal as expected.

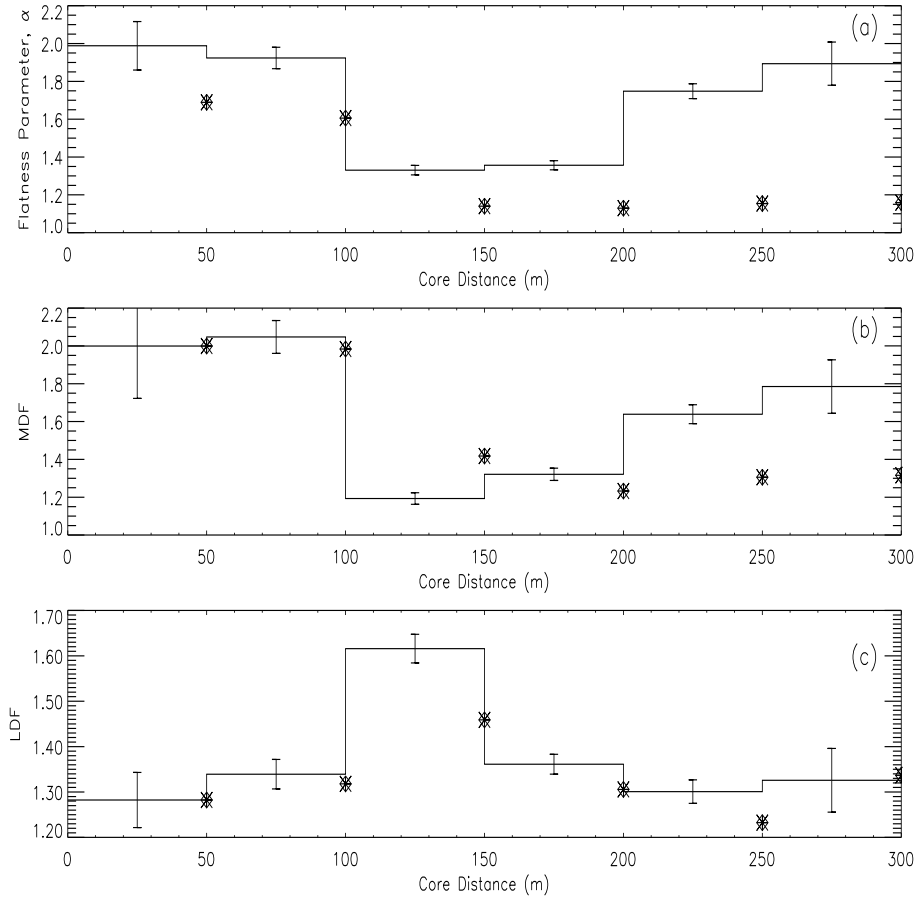


Figure 10. A plot showing the dependence of the three quality factors as a function of core distance cuts, both integral and differential. The histogram shows the differential core distance dependence of quality factors in units of 50 m for each of the parameters (a) α , (b) MDF and (c) LDF. The points (asterisks) show the quality factors when the core distances are chosen in the integral mode in units of 50 m. The quality factors are estimated for 500 GeV γ -rays and 1 TeV protons where 100 showers were simulated for each primary species.

al., 1989). After applying the cuts based on the three parameters, to the same data-set in tandem the resulting quality factors are 2.22 ± 0.06 , 1.53 ± 0.08 , 1.54 ± 0.10 for the three distinct primary energies studied here *viz.* 100 & 250 GeV, 0.5 & 1.0 TeV and 1.0 & 2.0 TeV respectively. Thus using the Čerenkov photon density based parameters alone one is able to reject more than 90% of background protons.

The parameter α has been used by the CELESTE group to reject nearly 80% of the proton primaries from their data from the Crab Nebula. From their simulation studies a quality factor of 1.6 has been

obtained while the γ -ray energy threshold of CELESTE is ~ 50 GeV. From the present studies we have estimated a quality factor of 1.33 for primary energies of 100 GeV and 250 GeV for γ -rays and protons respectively for Pachmarhi altitude (table 7. Considering their lower energy threshold (50 GeV), their quality factor is consistent with ours (De Naurois *et al.*, 2000).

9. Conclusions

In this work we have examined the feasibility of improving the signal to noise ratio using the differences in the fluctuations of Čerenkov photon distribution in the light pool generated by γ -ray and proton initiated showers. The estimates of quality factors are relevant to the configuration of PACT which uses the wavefront sampling technique. However the quality factors using the parameters studied here can be easily optimized to any array configuration of Čerenkov telescopes.

Various shower characteristics like the image shape, distribution of light on the ground, time profile & structure, spectrum, polarization and the UV content in the Čerenkov light have been suggested in the literature for hadron discrimination. It has been verified experimentally that the shape and orientation of the Čerenkov images can reject more than 99% of the background (Hillas , 1996). Similarly, from our earlier studies on Čerenkov photon temporal properties (Chitnis and Bhat , 2001) and the present investigations on their photometric properties we can conclude that one can efficiently reject more than 90% of the cosmic ray background while adopting wavefront sampling technique.

Acknowledgements

We would like to acknowledge the fruitful discussions with and helpful suggestions from Profs. K. Sivaprasad, P. R. Vishwanath and B. S. Acharya during the present work.

References

- Aharonian, F. A. *et al.*, 21st *Int. Cosmic Ray Conf.*, Adelaide (Australia), 4, 246, 1989.
- Aharonian, F. A. and Akerlof, C. W., *Ann. Rev. Nucl. Part. Sci.*, 47, 273, 1997.
- Aharonian, F. A. *et al.*, *High Energy Stereoscopic System*, letter of intent, Max Planck Institute for Nuclear Physics, Heidelberg, 1997.
- Aharonian, F. A. *et al.*, *Astrophys. J.*, 546, 898, 2001.

- Arqueros, F. *et al.*, *Towards a Major Atmospheric Čerenkov Detector - V*, Berg-en-Dal, Kruger National Park (South Africa), Ed: O. C. de Jager., p 240, 1997.
- Arqueros, F. *et al.*, *Astropart. Phys.*, 17, 293, 2002.
- Badran, H. M. and Weekes, T. C., *Astropart. Phys.*, 7, 307, 1997.
- Bhat, P. N., *High Energy Astronomy & Astrophysics*, Proc. of the Int. Colloquium to commemorate the Golden Jubilee year of *Tata Institute of Fundamental Research*, Ed: P. C. Agrawal and P. R. Vishwanath, University Press, 370, 1998.
- Blanch, O. *et al.*, *The MAGIC Telescope for gamma-ray astrophysics above 10-30 GeV*, letter of intent, Max Planck Institute for Physics, Munich, 1998.
- Bugayov, V. V. *et al.*, *Astropart. Phys.*, 17, 41, 2002.
- Catanese, M. and Weekes, T. C., 1999 *Publ. Astron. Soc. Pacific*, 111, 1193, 1999.
- Cawley, M F. and Weekes, T. C., *Experimental Astronomy*, 6, 7, 1995.
- “Celeste” proposal, <http://www.cenbg.in2p3.fr/Astroparticule>, 1996.
- Chitnis, V. R. and Bhat, P. N., *Astropart. Phys.* 9, 45, 1998.
- Chitnis, V. R. and Bhat, P. N., *Astropart. Phys.*, 12, 45, 1999.
- Chitnis, V. R. and Bhat, P. N., *Astropart. Phys.*, 15, 29, 2001.
- Chitnis, V. R. and Bhat, P. N., *Bull. Astr. Soc. India*, 30, 345, 2002.
- Cronin, J. W., Gibbs, K. G. and Weekes, T. C., *Ann. Rev. Nucl. Part. Sci.*, 43, 883, 1993.
- De Naurois, M. *et al.*, *AIP Conf. Proc.* (Ed. F. A. Aharonian and H. J. Volk), 558, 540, 2000.
- De Naurois, M. *et al.*, *Astrophys. J.*, 566, 343, 2002.
- Fegan, D. J., *J. Phys. G: Nucl. Particle Phys.*, 23, 1013, 1997.
- Ford, R. L. and Nelson, W. *SLAC Report # 210.*, 1978
- Heck, D. *et al.*, *Forschungszentrum Karlsruhe Report*, FZKA 6019, 1998.
- Hillas, A. M. and Patterson, J. R., *J. Phys. G: Nucl. Particle Phys.*, 16, 1271, 1990.
- Hillas, A. M., *Space Sci. Rev.*, 75, 175, 1996.
- Hofmann, W., Lampeitl, H., Konopelko, A. and Krawczynski, H., *Astropart. Phys.*, 12, 207, 2000.
- Knapp, J. and Heck, D., *EAS Simulation with CORSIKA, V5.60: A user's Guide.*, 1998.
- Linsley, J., *US Standard Atmosphere*, (US Govt. Printing Office, Washington), 1962.
- Majumdar, P. *et al.*, *Astropart. Phys.*, (in press); *Astro-ph/0204112*
- Nelson, W. R., *The EGS4 Code System, SLAC Report 265.*, 1985
- Ong, R., *et al.*, *Towards a Major Atmospheric Čerenkov Detector - IV*, Padova, Ed: M. Cresti, 261, 1995.
- Ong, R., *Il Nuovo Cim.*, 19, 971, 1996.
- Ong, R. and Covault, C. E., *Towards a Major Atmospheric Čerenkov Detector - V*, Berg-en-Dal, Kruger National Park (South Africa), Ed: O. C. de Jager., p 247, 1997.
- Ong, R., *Phys. Rep.*, 305, 93, 1998.
- Oser, S., *et al.*, *Astrophys. J.*, 547, 949, 2001.
- Rahman, M. A. *et al.*, *Experimental Astron.*, 11, 113, 2001.
- Rao, M. V. S. and Sinha, S., *J. Phys. G: Nucl. Particle Phys.*, 14, 811, 1988.
- Roberts, M. D., *et al.*, *J. Phys. G: Nucl. Particle Phys.*, 24, 225, 1998.
- Tümer, O. T. *et al.*, *Nucl. Phys. B (Proc. Suppl.)*, 14A, 351, 1990.
- Vishwanath, P. R., *Towards a Major Atmospheric Čerenkov Detector - II for TeV Astro/Particle Physics*, Calgary, (Canada), Ed: R. C. Lamb, 115, 1993.
- Weekes, T. C., *Physics Reports*, 160, 1, 1988.
- Weekes, T. C. *et al.*, *Astrophys. J.*, 342, 379, 1989.
- Weekes, T. C., *Space Sci. Rev.*, 75, 1, 1996a.

Weekes, T. C.*et al.*, *Very Energetic Radiation Imaging telescope Array System*, (VERITAS), proposal, Smithsonian Astrophysical Observatory, 1996b.